

Thermal Index of Neutron Stars in the Virial Approximation

Adriana Nadal Matosas

Facultat de Física, Universitat de Barcelona, Diagonal 645, 08028 Barcelona, Spain.

Advisor: Dr. Arnau Rios Huguet

In the era of gravitational waves detection, the need to understand matter at finite temperature has arisen. The thermal index describes the thermal effects in a neutron star's equation of state. In this work we use the virial equation of state of interacting nucleons and consider the contribution of electrons as an ideal Fermi gas. We compute the thermal index for neutron stars in conditions of low density and high temperature. We find that the thermal index ranges from $4/3$ to $5/3$, and is primarily sensitive to the isospin asymmetry of the system.

I. INTRODUCTION

Following the recent detection of gravitational waves emitted by the merger of two neutron stars (NSs) [1], the necessity to understand the thermodynamics of such objects has increased. To understand this phenomena, we need to numerically simulate the the merger of two NSs, which requires an understanding of the micro-physics of the system. The temperature of the NS during the merger is expected to raise to 10-100 MeV [2]. At such temperatures, thermal effects can make up a significant contribution to the thermodynamics of the system. Therefore, this phenomena can no longer be described by the equations of *cold* matter. Instead, we require a detailed knowledge of the equation of state (EOS) of *hot* matter, that is a relation between pressure, density and temperature that models the behaviour of matter under these extreme conditions.

At sufficiently high temperature, all clusters and isotopes found in a NS are expected to be unbound, and one expects a homogeneous gas of neutrons, protons and electrons should be an approximate model for matter in these conditions. We consider this gas to be in conditions of chemical equilibrium. The EOS for such gas has to successfully contemplate the properties of strong nuclear interactions between nucleons. In contrast, electrons interact rather weakly and can be treated as an ideal relativistic Fermi gas [3]. This has allowed us to derive the EOS of asymmetric matter for electrons and nucleons separately, using the virial expansion method to consider the nuclear interactions among the latter.

The thermal index, Γ_{th} , is the adiabatic index that describes the effect of finite temperature in the EOS and thus is key to developing numerical simulations of NS mergers [4]. In this work we derive the thermal index for neutron and asymmetric matter in β -equilibrium using the virial expansion method, which gives a reliable result for very low densities and temperatures. In Sec. II we present the virial expansion method, which we have applied to pure neutron matter in Sec. III A and further expanded to asymmetric matter in Sec. III B. Finally, in Sec. IV we present the conclusions drawn.

II. VIRIAL EQUATION OF STATE

The virial expansion method is a general, model-independent framework to incorporate strong interactions between nucleons in the EOS of a *hot* dilute gas [5]. The virial EOS is obtained by expanding the pressure in a power series of the fugacity, $z = e^{\mu/T}$ [6], where μ is the chemical potential,

$$P = \frac{T}{\lambda^3} \sum_{n=1}^{\infty} b^{(n)} z^n \quad (1)$$

For this equation, and throughout the entire work, we have considered $k_B = 1$. Here $\lambda = \hbar(2\pi/mT)^{1/2}$ is the nucleon thermal wavelength and $b^{(n)}$ is the n th virial coefficient. This expansion is valid on the condition that z is small, which implies that the expansion is valid for very low densities. An additional assumption that has to be made is that the system is in a gas phase and has undergone no phase transition with decreasing temperature or increasing density.

The n th virial coefficient captures the thermodynamics of the n -body systems, consisting in a non-interacting term, associated to the free Fermi gas contribution, $b_0^{(n)} = (-1)^{n+1} n^{-5/2}$, and an interaction-induced term, $\Delta b^{(n)}$. This interacting term considers any possible n -body clusters that may be relevant in the conditions studied, as well as the scattering phase shifts. It is temperature dependent, but it is independent on density [5].

To meet the requirements for a valid virial EOS, we have conducted the study of the thermal index in conditions of low density and high temperature. To study a homogeneous gas of neutrons, protons and electrons, we have chosen the range of 1 – 25 MeV for temperature and $10^{-5} - 10^{-1} \text{ fm}^{-3}$ for density. Furthermore, we have verified that $z < 0.5$ for all data. For these conditions of temperature and density, the only relevant bound-state that we consider in the interacting terms of the virial coefficients is the deuteron. That is because at high temperatures and high levels of asymmetry the presence of alpha particles and other clusters is not expected to be significant [7].

III. THERMAL INDEX OF A NEUTRON STAR

The EOS for any gas consists of a *cold* term, the contribution to the thermodynamics of the system for $T = 0$, and an additional *hot* term, for $T \neq 0$.

$$P(n, T) = P(n, T = 0) + P_{th}(n, T) \quad (2)$$

with n the number of particles for unit of volume and $P_{th}(n, T)$ the thermal contribution to the pressure. The energy density of the gas follows the same structure, $\epsilon(n, T) = \epsilon(n, T = 0) + \epsilon_{th}(n, T)$, with $\epsilon_{th}(n, T)$ its thermal contribution. The thermal effects in the EOS are expressed in terms of the thermal index, which is obtained from the thermal pressure and thermal energy density as [4]

$$\Gamma_{th} = 1 + \frac{P_{th}}{\epsilon_{th}}. \quad (3)$$

The thermal index is often considered to be constant and approximately consistent with an ideal-fluid EOS, $\Gamma_{th} = \frac{5}{3}$. However, Γ_{th} is expected to have a strong density dependence for degenerate matter, such as the one found in NS cores [8].

A. Neutron Matter

First we consider a pure neutron gas, which is expected to be a good approximation of NS matter. This allows us to analyse the effects of nucleon interactions without the contribution of leptons. We derive its virial EOS as a power series of the fugacity as explained in Sec. II, obtaining

$$P = \frac{2T}{\lambda^3} [z + z^2 b_n^{(2)} + z^3 b_n^{(3)} + O(z^4)], \quad (4)$$

where $b_n^{(2)}$ and $b_n^{(3)}$ are the second and third virial coefficients for neutron matter respectively. For this section, all expressions have been derived up to third order in the fugacity, z .

The second virial coefficient, $b_n^{(2)}$, is directly related to the two-body elastic scattering phase shifts. The interacting term $\Delta b_n^{(2)}$ is calculated following

$$\Delta b_n^{(2)}(T) = \frac{1}{\sqrt{2\pi T}} \int_0^\infty e^{-E/2T} \delta^{tot}(E) dE \quad (5)$$

where $\delta^{tot}(E)$ is the sum of the isospin-triplet elastic scattering phase shifts at laboratory energy E . This sum is over all partial waves allowed by spin statistics, with two-particle spin S and angular momentum L . It includes a degeneracy factor depending on the total angular momentum, J ,

$$\begin{aligned} \delta^{tot}(E) &= \sum_{S,L,J} (2J+1) \delta_{2S+1LJ}(E) \\ &= \delta_{1S_0} + \delta_{3P_0} + 3\delta_{3P_1} + 5\delta_{3P_2} + 5\delta_{1D_2} + \dots \end{aligned} \quad (6)$$

Adding the non-interacting term, the second virial coefficient becomes

$$b_n^{(2)}(T) = \frac{1}{\sqrt{2\pi T}} \int_0^\infty e^{-E/2T} \delta^{tot}(E) dE - 2^{-5/2}. \quad (7)$$

The third virial coefficient, $b_n^{(3)}$, is included to make an error estimate of the results. This coefficient captures the thermodynamics of the three-body interacting system, its calculation has only been achieved for a unitary gas (a strongly interacting gas with an infinite scattering length). Assuming the ratio between interacting terms of the second and third virial coefficient for the unitary gas, $\Delta b_{unit}^{(3)}/\Delta b_{unit}^{(2)} = -0.5022$ [9], is the same in a neutron Fermi gas, we can estimate the value of $b_n^{(3)}$,

$$b_n^{(3)} = 3^{-5/2} + \Delta b_n^{(3)} = 3^{-5/2} - 0.5022 \Delta b_n^{(2)}. \quad (8)$$

The density is obtained by differentiating the pressure with respect to the fugacity, $n = z/T(\partial_z P)_{V,T}$, giving

$$n = \frac{2}{\lambda^3} [z + 2z^2 b_n^{(2)} + 3z^3 b_n^{(3)}]. \quad (9)$$

The entropy density can be obtained by differentiating the pressure with respect to temperature, $s = (\partial_T P)_\mu$, which yields

$$s = \frac{5}{2} \frac{P}{T} - n \log z + \frac{2T}{\lambda^3} [z^2 b_n^{(2)'} + z^3 b_n^{(3)'}], \quad (10)$$

where $b_n^{(m)'} = \partial_T b_n^{(m)}$ is the temperature derivative of the n th-virial coefficient. Finally, the energy density is calculated from the entropy density and the pressure, $\epsilon = Ts + n\mu - P$, leading to

$$\epsilon = \frac{3}{2} P + \frac{2T^2}{\lambda^3} [z^2 b_n^{(2)'} + z^3 b_n^{(3)'}]. \quad (11)$$

By looking at Eq. (4) and (11), and comparing them to Eq. (2), we see that both the pressure and energy in the virial approximation are intrinsically thermal. Therefore, $P_{th} = P$ and $\epsilon_{th} = \epsilon$. The thermal index is hence calculated up to second order of the fugacity using the pressure and the energy density we derived, resulting in

$$\Gamma_{th} = \frac{5}{3} - \frac{4}{9} \Gamma^{(1)} z + \frac{4}{9} \Gamma^{(2)} z^2 \quad (12)$$

With $\Gamma^{(1)} = T b_n^{(2)'}$ and $\Gamma^{(2)} = \frac{2}{3} T b_n^{(2)'} - b_n^{(2)} + 0.5022$.

Observing Eq. (12), we expect Γ_{th} to approach the non-interacting limit for a very dilute gas of non-relativistic neutrons, $\Gamma_{th} \rightarrow \frac{5}{3}$ as $z \rightarrow 0$. By looking at the numerical values calculated of the virial coefficients, found in table (I) in the Appendix A, we note that $|\Gamma^{(1)}| < |\Gamma^{(2)}|$, but both add negative contributions to Γ_{th} for all temperatures. Taking this into consideration, we expect the thermal index to decrease as density increases.

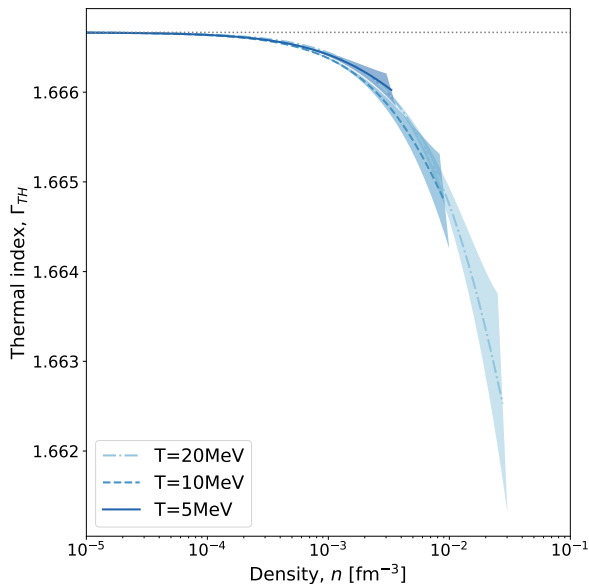


FIG. 1: Thermal index of neutron matter as a function of density, for $T = 5, 10$ and 20 MeV. The shaded area shows the error, estimated by incorporating $\pm b_n^{(3)}$. A grey dotted line shows the value of Γ_{th} in the non-interacting limit, for reference. For all data shown, the fugacity is $z < 0.5$.

Figure (1) shows the dependence in density of the thermal index for $T = 5, 10$ and 20 MeV. Each line represents the evolution of the thermal index for a given temperature, calculated with thermal pressure (Eq. (4)) and energy (Eq. (11), up to second order in the fugacity). The error is shown as the shaded area around each line, with its limits introducing the estimated correction of $\pm b_n^{(3)}$. We have added a grey dotted line for the value of Γ_{th} in the non-interacting limit, for reference.

We observe that the thermal index is relatively independent of the temperature in the region studied. As expected for small densities, the value of the thermal index approaches the non-interacting value, following the behaviour of a non-relativistic ideal gas. As density increases, the contribution of the interaction results in a decrease of the thermal index. The value of the thermal index remains nearly unchanged, having decreased under a 0.3% for all temperatures considered. It can also be seen that the relative error estimated with the third virial coefficient is no more than 0.1%. In the following, we do not take the error into account and limit our discussion to the second order in z .

B. Asymmetric Matter

Now we consider a low density gas of interacting neutrons and protons, and free electrons. Beta decay and electron capture reactions are expected to be in chemical equilibrium [10],



This leads to an equality between their masses, m_τ and chemical potentials, μ_τ , where $\tau = n, p, e$. The equality follows

$$\mu_n + m_n = \mu_p + m_p + \mu_e + m_e \quad (15)$$

To ensure neutrality of charge, the constraint that both proton and electron densities must be equal, $n_p = n_e$, is added. Therefore, for each density and temperature the proportion of neutrons, protons and electrons at equilibrium is found solving these two equations. The relevant parameter is the proton fraction, $x_p = \frac{n_p}{n}$, since it states the level of asymmetry of the gas. Here n is the total baryon density, $n = n_n + n_p$

1. Electrons: ideal Fermi gas

As stated above, the electrons are considered as an ideal relativistic Fermi gas. Therefore, the *hot* EOS for the non-interacting gas of electrons is easily found. Starting from the zero-temperature chemical potential [3],

$$\mu_e = (3\pi^2 n x_p)^{1/3} \hbar c, \quad (16)$$

the expression for the thermal pressure can be found from a power series in T/mu_e , yielding

$$P_{th}^e = \frac{\mu_e^4}{12(\hbar c)^3} \left[2 \left(\frac{T}{\mu_e} \right)^2 + \left(\frac{7\pi^2}{5} - \frac{m_e^2 c^4}{2T^2} \right) \left(\frac{T}{\mu_e} \right)^4 \right]. \quad (17)$$

For an ideal relativistic gas, $P_{th}^e/\epsilon_{th}^e = 1/3$, therefore, $\epsilon_{th}^e = 3P_{th}^e$. These expressions are valid provided T/μ_e is small. To find their validity limit, we consider $T \approx \mu_e$. For each temperature and proton fraction the approximation breaks below $n = 8.8 \times 10^{-6} \left(\frac{0.5}{x_p} \right) \left(\frac{T}{10 \text{ MeV}} \right)^3 \text{ fm}^{-3}$.

2. Baryonic matter

To obtain the virial EOS for baryonic matter, expanding the procedure of Sec. II to protons, we obtain the pressure as power series in the fugacities, $z_n = e^{\mu_n/T}$ and $z_p = e^{\mu_p/T}$ for neutrons and protons respectively.

$$P = \frac{2T}{\lambda^3} [z_n + z_p + (z_n^2 + z_p^2)b_n^{(2)} + 2z_n z_p b_{np}^{(2)} + O(z^3)] \quad (18)$$

where $b_{np}^{(2)}$ is the second virial coefficient for np interaction and $b_n^{(2)}$ is the second virial coefficient for nn and pp interactions. We consider the last two equivalent by neglecting the Coulomb interaction and assuming charge-independent nuclear interactions.

The coefficient $b_n^{(2)}$ is obtained as described in Eq. (7). The coefficient $b_{np}^{(2)}$ can be decomposed in the neutron second virial coefficient, $b_n^{(2)}$, and the second virial coefficient for symmetric matter, $b_{nuc}^{(2)}$, following $b_{np}^{(2)}(T) = b_{nuc}^{(2)}(T) - b_n^{(2)}(T)$.

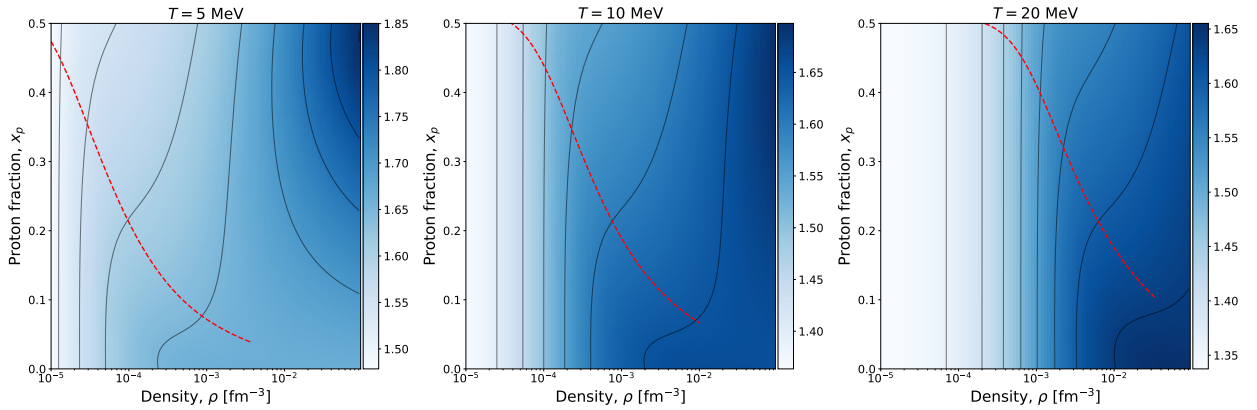


FIG. 2: Thermal index of NS as a function of density, n , and the proton fraction, x_p , for $T = 5, 10$ and 20 MeV. The dashed red line shows the path followed by the β -equilibrium. Each plot shows the range of densities in which the virial EOS is valid, with both fugacities obeying $z_n, z_p < 0.5$

To obtain $b_{nuc}^{(2)}$, the deuteron is considered as a bound-state contribution with an experimental binding energy of $E_d = 2.22$ MeV [7]. This contribution, together with the scattering phase-shifts gives

$$b_{nuc}^{(2)}(T) = \frac{3}{\sqrt{2}} \left(e^{E_d/T} - 1 \right) - 2^{-5/2} + \frac{1}{2^{3/2}\pi T} \int_0^\infty e^{-E/2T} \delta_{nuc}^{tot}(E) dE - 2^{-5/2}, \quad (19)$$

where δ_{nuc}^{tot} is now the sum over all partial waves and includes degeneracy factors depending on the isospin, T , and the total angular momentum, J ,

$$\begin{aligned} \delta_{nuc}^{tot}(E) &= \sum_{S,L,J} (2J+1)(2T+1) \delta_{2S+1LJ}(E) \\ &= 3\delta_{1S_0} + 3\delta_{3S_1} + 3\delta_{1P_1} + 3\delta_{3P_0} + \dots \end{aligned} \quad (20)$$

Each density, n_n and n_p for neutrons and protons respectively, is obtained by differentiating the pressure with respect to their fugacity, $n_\tau = z_\tau / T (\partial_{z_\tau} P)_{V,T}$, giving

$$n_\tau = \frac{2}{\lambda^3} \left[z_\tau + 2z_\tau^2 b_n^{(2)} + 2z_n z_p b_{np}^{(2)} \right], \quad (21)$$

with $\tau = n, p$. The entropy density is obtained by differentiating the pressure with respect to temperature, $s = (\partial_T P)_{\mu_n, \mu_p}$, resulting in

$$s = \frac{5P}{2T} - n_n \log z_n - n_p \log z_p + \frac{2T}{\lambda^3} \left[(z_n^2 + z_p^2) b_n^{(2)'} + 2z_n z_p b_{np}^{(2)'} \right] \quad (22)$$

Finally, the energy density is calculated from the entropy density and the pressure, $\epsilon = Ts + \sum_{i=n,p} n_i \mu_i - P$, leading to

$$\epsilon = \frac{3}{2}P + \frac{2T^2}{\lambda^3} \left[(z_n^2 + z_p^2) b_n^{(2)'} + 2z_n z_p b_{np}^{(2)'} \right]. \quad (23)$$

Like in Sec. III A, looking at Eq. (18) and (23), and comparing them to Eq. (2), we see that both the pressure and energy of the system are intrinsically thermal. Therefore, $P_{th}^{nuc} = P$ and $\epsilon_{th}^{nuc} = \epsilon$. Adding the contribution of the electrons, the thermal index is calculated using the pressures and the energy densities we just derived.

$$\Gamma_{th} = 1 + \frac{P_{th}^{nuc} + P_{th}^e}{\epsilon_{th}^{nuc} + \epsilon_{th}^e} \quad (24)$$

Figure (2) shows the thermal index as a function of density and isospin asymmetry for three different panels: $T = 5$ (left panel), 10 (central panel) and 20 MeV (right panel). Red dashed lines show the path followed by the β -equilibrium at each temperature. The composition of a NS evolves consistently with the increase of temperature. At low densities it tends to symmetric matter ($x_p \approx 0.5$), and it approaches purely neutron matter ($x_p \approx 0$) as density increases. This regime shift is clearly observed in the evolution of the thermal index.

Figure (3) shows the dependence on nuclear interactions of the thermal index. It shows the evolution of Γ_{th} against the density for $T = 5, 10$ and 20 MeV. Solid lines correspond to interacting results whereas dashed lines show the non-interacting case. Two grey dotted lines have been added to indicate the values associated to the relativistic and the non-relativistic ideal gases.

In contrast with the results obtained for neutron matter, we observe a dependence with temperature in the thermal index. However, Γ_{th} increases with density in a similar way for all temperatures. There is an inflection point that divides this behaviour in two regimes. At lower densities, the thermal contributions of the electrons dominate over those of the nucleons, resulting in a thermal index not far from the limit of a relativistic Fermi gas, $\Gamma_{th} \approx \frac{4}{3}$. As density increases, the value approaches the limit for pure neutron matter, a non-relativistic ideal gas, $\Gamma_{th} \approx \frac{5}{3}$.

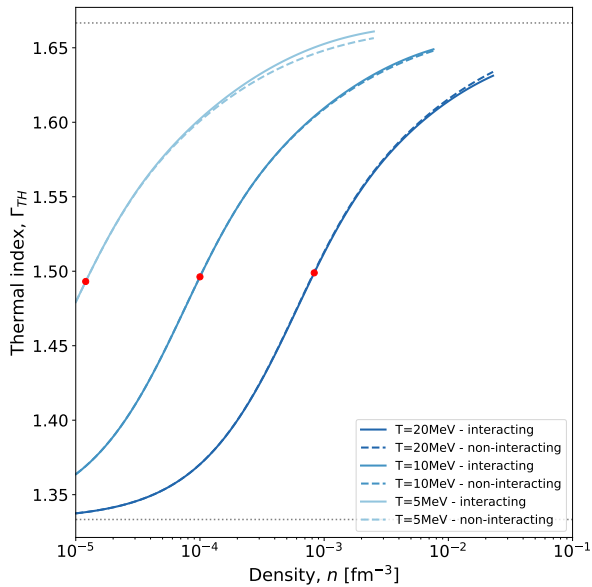


FIG. 3: Thermal index of neutron-star matter as a function of density, for $T = 5, 10$ and 20 MeV. For each temperature, a solid line shows the thermal index of asymmetric matter in β -equilibrium considering interactions. A dashed line shows the thermal index in the non-interacting limit. Grey dotted lines show the values of Γ_{th} in both the relativistic and the non-relativistic limits. Red dots show the estimated density at the inflexion point. All data shown complies $z < 0.5$.

Figure (3) also shows, in the form of a red dot, the density at which this regime shift is expected to occur. This value can be estimated considering $P_{th}^e \approx P_{th}^{nuc}$ and $x_p \approx 0.5$, obtaining a value of $n = 10^{-4} \left(\frac{T}{10 \text{ MeV}}\right)^3 \text{ fm}^{-3}$.

The effect of interactions is consistent with the results in Sec. III A for $T > 10$ MeV, as they decrease the value of the thermal index when density increases. Although considering interactions provide a 9% (10%) modification in P_{th} (ϵ_{th}), they only decrease Γ_{th} by 0.3%. Their effect is once again negligible.

IV. CONCLUSIONS

In order to study the thermal index of a NS we have considered a homogeneous gas of diluted neutrons, protons and electrons at high temperature. We have treated the electrons as a relativistic free gas and have included the nucleon interactions through the virial coefficients.

Using this method, we have seen the quantitative effect that nuclear interactions have in the thermodynamics of a *hot* NS. For both pure neutron matter and asymmetric matter we have found that, the effect interactions have on the thermal index are of the order of 0.3%. We have also estimated the error, found to be of the order of 0.1%.

Furthermore we have studied the dependence of Γ_{th} with density. We have found that, although nuclear interactions don't seem to have a big effect on the thermal index, the system's isospin asymmetry is key to determine its value. We have found the thermal index of a low density NS ranges from $\Gamma_{th} = \frac{4}{3}$ to $\frac{5}{3}$, smoothly evolving from an electron-dominated phase at low densities to a neutron-dominated phase as density increases.

These results can be applied to simulate the merger of NS, now contemplating the dependence of the thermal index with density, temperature and isospin asymmetry. To further extend the study on the thermal index, the interaction of electrons and the presence of other bound states, such as alpha particles [7], could be considered to verify the significance of their contributions. Additionally, to expand the range of temperature, the presence of pions could be included.

Acknowledgments

I would like to thank Dr. Arnau Rios, not only for his guidance along this project, but also for making it an exciting and rewarding experience. I would also like to thank my family and friends for all the support.

-
- [1] B.P. Abbott et al. (LIGO Scientific Collaboration and Virgo Collaboration). Gw170817: Observation of gravitational waves from a binary neutron star inspiral. *Phys. Rev. Lett.*, 199:161101, Oct. 2017.
 - [2] F. Özel C. A. Raithel and D. Psaltis. Finite-temperature extension for cold neutron star equations of state. *ApJ*, 875:018039, Apr. 2019.
 - [3] J. M. Lattimer and F. Douglas Swesty. A generalized equation of state for hot, dense matter. *Nuc. Phys. A*, 535:331376, Jun. 1991.
 - [4] A. Carbone and A. Schwenk. Ab initio constraints on thermal effects of the nuclear equation of state. *Phys. Rev. C*, 100:025805, Aug. 2019.
 - [5] C.J. Horowitz and A. Schwenk. The virial equation of state of low-density neutron matter. *Phys. Lett. B*, 638:153159, Jul. 2006.
 - [6] K. Huang. *Statistical Mechanics*. John Wiley & Sons, Inc, 2 edition, 1928.
 - [7] C.J. Horowitz and A. Schwenk. Cluster formation and the virial equation of state of low-density nuclear matter. *Nuc. Phys. A*, 776:055079, Sept. 2006.
 - [8] V. Paschalidis C. A. Raithel and F. Özel. Realistic finite-temperature effects in neutron star merger simulations. *Phys. Rev. D*, page 063016, Sept. 2021.
 - [9] Y. Hou and J. E. Drut. Fourth- and fifth-order virial coefficients from weak coupling to unitarity. *Phys. Rev. Lett.*, page 050403, Jul. 2020.
 - [10] K.S. Krane. *Introductory Nuclear Physics*. John Wiley Sons, New York, 2 edition, 1988.
 - [11] R. Navarro Pérez, J. E. Amaro, and E. Ruiz Arriola. Partial-wave analysis of nucleon-nucleon scattering below the pion-production threshold. *Phys. Rev. C*, 88:024002, Aug 2013.

Appendix A: Numerical values of the virial coefficients

T [MeV]	$b_n^{(2)}$ (with CIB)	$Tb_n^{(2)'} \equiv \Gamma^{(1)}$	$b_{np}^{(2)}$	$Tb_{np}^{(2)'}$	$b_{nuc}^{(2)}$	$Tb_{nuc}^{(2)'}$	$\Gamma^{(2)}$
1	0.2514	0.0389	19.3522	-43.5383	19.6037	-43.4994	-0.2248
2	0.2723	0.0176	6.1185	-7.3684	6.3908	-7.3508	-0.2182
3	0.2782	0.0085	4.0329	-3.5351	4.3111	-3.5266	-0.2183
4	0.2807	0.0046	3.2099	-2.3074	3.4906	-2.3029	-0.2185
5	0.2821	0.0034	2.7636	-1.7314	3.0457	-1.7280	-0.2178
6	0.2832	0.0037	2.4795	-1.4031	2.7627	-1.3994	-0.2165
7	0.2844	0.0048	2.2801	-1.1926	2.5645	-1.1878	-0.2146
8	0.2855	0.0064	2.1309	-1.0464	2.4164	-1.0400	-0.2124
9	0.2866	0.0083	2.0140	-0.9392	2.3006	-0.9309	-0.2100
10	0.2878	0.0104	1.9194	-0.8572	2.2072	-0.8469	-0.2075
11	0.2890	0.0123	1.8407	-0.7926	2.1297	-0.7802	-0.2050
12	0.2903	0.0142	1.7739	-0.7403	2.0642	-0.7261	-0.2025
13	0.2916	0.0158	1.7163	-0.6973	2.0079	-0.6814	-0.2000
14	0.2930	0.0173	1.6659	-0.6613	1.9589	-0.6440	-0.1977
15	0.2944	0.0186	1.6212	-0.6308	1.9156	-0.6123	-0.1955
16	0.2958	0.0196	1.5813	-0.6048	1.8770	-0.5851	-0.1933
17	0.2971	0.0205	1.5452	-0.5823	1.8423	-0.5617	-0.1914
18	0.2984	0.0212	1.5124	-0.5628	1.8108	-0.5416	-0.1896
19	0.2997	0.0218	1.4823	-0.5458	1.7820	-0.5240	-0.1880
20	0.3009	0.0222	1.4546	-0.5309	1.7555	-0.5087	-0.1865
21	0.3021	0.0224	1.4289	-0.5178	1.7310	-0.4954	-0.1852
22	0.3032	0.0225	1.4050	-0.5062	1.7082	-0.4837	-0.1840
23	0.3043	0.0224	1.3826	-0.4961	1.6869	-0.4737	-0.1830
24	0.3053	0.0221	1.3616	-0.4871	1.6669	-0.4649	-0.1822

TABLE I: Numerical values of the second virial coefficients for both neutron and nucleon interactions, calculated following Eq. (7) and (19), using the Granada database phase shifts for energies up to 350 MeV [11]. The second virial coefficient for neutron interactions takes into account the effects due to charge-independence breaking (CIB). The coefficients $\Gamma^{(1)}$ and $\Gamma^{(2)}$ from Eq. (12) are also shown.